Time-Dependent System Reliability Analysis Using Random Field Discretization

Zhen Hu
Department of Civil and Environmental Engineering,
Vanderbilt University,
279 Jacobs Hall,
VU Mailbox: PMB 351831,
Nashville, TN 37235
e-mail: zhen.hu@vanderbilt.edu

Sankaran Mahadevan
Professor
Department of Civil and Environmental Engineering,
Vanderbilt University,
272 Jacobs Hall,
VU Mailbox: PMB 351831,
Nashville, TN 37235
e-mail: sankaran.mahadevan@vanderbilt.edu

This paper proposes a novel and efficient methodology for time-dependent system reliability analysis of systems with multiple limit-state functions of random variables, stochastic processes, and time. Since there are correlations and variations between components and over time, the overall system is formulated as a random field with two dimensions: component index and time. To overcome the difficulties in modeling the two-dimensional random field, an equivalent Gaussian random field is constructed based on the probability equivalency between the two random fields. The first-order reliability method (FORM) is employed to obtain important features of the equivalent random field. By generating samples from the equivalent random field, the time-dependent system reliability is estimated from Boolean functions defined according to the system topology. Using one system reliability analysis, the proposed method can get not only the entire time-dependent system probability of failure curve up to a time interval of interest but also two other important outputs, namely, the time-dependent probability of failure of individual components and dominant failure sequences. Three examples featuring series, parallel, and combined systems are used to demonstrate the effectiveness of the proposed method. [DOI: 10.1115/1.4031337]

Keywords: time-dependent reliability, system reliability, stochastic processes, random field

1 Introduction

This paper focused on time-dependent reliability, due to time-variant loads, degradation of material strength, wear, etc. Time-dependent reliability is defined as the probability that there is no failure over a time period of interest. This definition considers both variations in the operating environment and system characteristics over time.

Significant efforts have been reported regarding methods for time-dependent component and system reliability analyses. For time-dependent component reliability analysis, the available reliability analysis methods can be roughly classified into three groups: upcrossing rate methods, analytical methods without using the upcrossing rate, and the sampling-based methods. Examples of the upcrossing rate methods include the PHI2 method developed by Andrieu-Renaud et al. [1], the upcrossing rate method [2], the joint upcrossing rate method [3], and many other empirical modifications made to the upcrossing rate method [4]. Efforts have also been made to remove the limitations of upcrossing rate methods by analyzing the extreme response. Examples include the composite limit-state function method [5], extreme value response surface method [6,7], extreme value distribution method based on the probability density evolution [8], stochastic process discretization method [9], and envelope function method [10]. Methods falling into the third group are the adaptive importance sampling approach [11], Markov chain Monte Carlo simulation [12], and first-order sampling approach [13].

The time-dependent system reliability analysis is much more complicated than the time-dependent component reliability analysis. Methods have been proposed for time-dependent system reliability analysis based on assumptions and simplifications. For instance, Hagen and Tvedt proposed an upcrossing rate method for time-dependent system reliability analysis by bounding the system response based on combinations of bivariate responses [14]. Song and Der Kiureghian developed a joint first-passage probability method based on the conditional distribution analysis [15]. Based on the integration of Monte Carlo simulation (MCS) and asymptotic extreme value theory, Radhika et al. developed a reliability analysis method for nonlinear vibrating systems [16]. Dey and Mahadevan developed an adaptive importance sampling approach for system reliability analysis with multiple failure sequences, considering both ductile and brittle failures of components in mechanical systems [17].

In order to efficiently and accurately estimate the time-dependent system reliability and remove the assumptions and simplifications (Poisson assumption, simplification of system topology) used in most of the current methods, an efficient method is developed in this paper based on the concept of random field discretization. It is an extension of the method developed in Ref. [13]. The advantages of the developed method are threefold. First, it is applicable for general problems with random variables, stochastic processes, and time. The Poisson assumption used in the upcrossing rate method is completely removed. Second, using one reliability analysis, the proposed method obtains not only the time-dependent reliability over a specific time interval but also the entire time-dependent probability of failure curve up to that time interval. Third, without requiring extra computational effort, the time-dependent reliability of the individual components and the dominant failure sequences are obtained as byproducts of time-dependent system reliability analysis.

The remainder of this paper is organized as follows. Section 2 reviews the background of system reliability analysis and time-dependent system reliability analysis. Section 3 develops the proposed new method for time-dependent system reliability analysis. Following this, algorithmic implementation of the proposed method is discussed in Sec. 4. Three numerical examples are given in Sec. 5. Conclusions are drawn in Sec. 6.

2 Background of Time-Dependent System Reliability Analysis

2.1 System Reliability Analysis. Engineering systems can be grouped into three categories based on the system topology: series

Contributed by the Design Automation Committee of ASME for publication in the Journal of Mechanical Design. Manuscript received April 29, 2015; final manuscript received August 11, 2015; published online September 2, 2015. Assoc. Editor: Xiaoping Du.

systems, parallel systems, and combined systems. Let $\mathbf{X}$ be a vector of random inputs of a system and $g_i(\mathbf{X})$ be the limit-state function of component i. The time-independent probabilities of failure for series and parallel systems with n components are given by

$$p_f^{\text{series}} = \Pr\{\bigcup_i g_i(\mathbf{X}) > 0\} \quad (1)$$

$$p_f^{\text{parallel}} = \Pr\{\bigcap_i g_i(\mathbf{X}) > 0\} \quad (2)$$

in which $i = 1, 2, \cdots, n$ are indices of the components, $g_i(\mathbf{X}) > 0$ defines the failure event, $\Pr\{\cdot\}$ stands for probability, "$\cup$" is union, and "$\cap$" is intersection.

For the combined systems, the expression of probability of failure will vary with the system topology. In problems where the limit-state function evaluations require expensive computer simulation models, directly solving Eqs. (1) and (2) is difficult. Methods have been proposed to approximate the probabilities given in the above equations, for example, bounding formulas developed by Ditlevsen [18], multiple linearization [19], importance sampling [20], the complementary intersection method [21], and the integrated performance measure approach [22]. All these methods are developed for time-independent reliability analysis.

2.2 Time-Dependent System Reliability Analysis. Let $\mathbf{Y}(t)$ be a vector of stochastic loads, realizations of which vary with time and are correlated over time. The limit-state function for component i becomes

$$G_i(t) = g_i(\mathbf{X}, \mathbf{Y}(t), t) \quad (3)$$

For a time period of interest $[t_0, t_e]$, where t_0 is the initial time instant and t_e is the final time instant, the time-dependent probability of failure of component i is given by

$$p_f^i(t_0, t_e) = \Pr\{g_i(\mathbf{X}, \mathbf{Y}(t), t) > 0, \exists t \in [t_0, t_e]\} \quad (4)$$

where " $\exists$ " means "there exists."

After introducing the time-dependent factors into the limit-state functions, the system probabilities of failure given in Eqs. (1) and (2) are rewritten as follows:

$$p_f^{\text{series}}(t_0, t_e) = \Pr\{\bigcup_i g_i(\mathbf{X}, \mathbf{Y}(t_i), t_i) > 0, \exists t_i \in [t_0, t_e]\} \quad (5)$$

$$p_f^{\text{parallel}}(t_0, t_e) = \Pr\{\bigcap_i g_i(\mathbf{X}, \mathbf{Y}(t_i), t_i) > 0, \exists t_i \in [t_0, t_e]\} \quad (6)$$

The above equations can also be written in terms of global extreme values as

$$p_f^{\text{series}}(t_0, t_e) = \Pr\{\bigcup_i G_i^{\max} = \max_{t_i \in [t_0, t_e]} [g_i(\mathbf{X}, \mathbf{Y}(t_i), t_i)] > 0\} \quad (7)$$

$$p_f^{\text{parallel}}(t_0, t_e) = \Pr\{\bigcap_i G_i^{\max} = \max_{t_i \in [t_0, t_e]} [g_i(\mathbf{X}, \mathbf{Y}(t_i), t_i)] > 0\} \quad (8)$$

Due to the involvement of correlations over time and global optimizations (if Eqs. (7) and (8) are used), estimating the time-dependent system failure probability is much more complicated than estimating time-independent system failure probability. Although methods have been proposed based on the assumptions and simplifications, such as the Poisson process assumption [17] and bounding formulas [14], accurate and efficient estimation of the time-dependent system probability of failure is still a challenging issue. In Sec. 3, we present a new method for time-dependent system reliability analysis, which is able to approximate the time-dependent probability of failure accurately and efficiently if the FORM is applicable for the instantaneous component reliability analysis.

3 Time-Dependent System Reliability Analysis Using Random Field Discretization

Reliability analysis from the random field discretization perspective has been investigated by Hu and Du [13] for the time-dependent component reliability analysis. Here, we further extend the idea to time-dependent system reliability analysis. In this section, we first provide an overview of the proposed method. After this, detailed implementation procedures are explained.

3.1 Overview of the Proposed Method. As indicated in Fig. 1, a typical time-dependent system reliability analysis problem can be decomposed into a three-level analysis problem. The three levels are: level one—component-level analysis with uncertain inputs, level two—system-level response modeling, and level three—reliability analysis based on the system topology and system response modeling. Since the component-level analysis usually relies on computer simulations, how to reduce the computational effort spent on the level one analysis has been an active research topic. Most of the system reliability analysis methods implement an integrated framework, in which lower level analyses are affected by the higher level analysis method [15]. In the integrated framework, the complexity of the system reliability analysis will increase with the complexity of any of the three levels. For instance, a system with complicated topology (level three) will make the overall system reliability analysis complicated even if the component-level analysis (level one) is simple. Since the level one analysis (time-dependent component reliability analysis) is already computationally intensive (if finite-element simulation is employed), solving the three levels together for time-dependent system reliability analysis is very challenging.

In this paper, we perform the three levels of analyses separately. The system response is modeled as a random field based on the component-level analysis. The component-level analyses (level one) are performed only at some specific time instants required by the system-level random field modeling (level two). Based on the random field modeling, the reliability analysis is conducted based on the system topology (level three) to estimate the time-dependent system reliability. Since the component-level analysis (level one) at specific time instants is a time-instantaneous reliability analysis problem, it has been intensively studied during the past decades. In this paper, we mainly focus on the level two analysis (system-level random field modeling). It is a critical part of the time-dependent system reliability analysis since it is a connection between the level one and three analyses. In Sec. 3.2, we will discuss why the system response can be modeled as a random field and how it can be accomplished.

3.2 System Response as a Random Field. A random field is defined over a parameter space of dimensionality at least once.

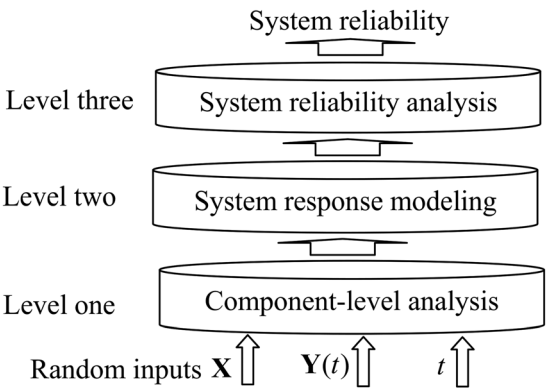

Fig. 1 Three-level illustration of time-dependent system reliability analysis

The term "field" is used when modeling stochastic variability over space, and the term "process" is used when modeling stochastic variability over time. For a random field $F(\mathbf{x}, \theta)$, where $\mathbf{x}$ are dimensional parameters and θ denotes the randomness of the field, $F(\mathbf{x}^{(i)}, \theta)$ is a random variable for any given point, $\mathbf{x}^{(i)}$. For any given θ^*, $F(\mathbf{x}, \theta^*)$ is a realization of $F(\mathbf{x}, \theta)$.

Assume that there are n components in a system with limit-state functions given by $G_i(t) = g_i(\mathbf{X}, \mathbf{Y}(t), t)$, $i = 1, 2, \ldots, n$. It is clear that $G_i(t)$ is a random variable at a specific time instant t. The response of the n-component system therefore consists of n correlated random variables. Considering both time and component index as coordinates, the overall system response $\tilde{G}$ is a two-dimensional random field. That is, the response $\tilde{G}$ is a random variable for any given values of component index i and time instant t. Fixing the time at a specific time instant, the system is a discrete random field with component index as the dimensional parameter. Fixing the component index, the system is a continuous random field (i.e., stochastic process) with time as the dimensional parameter. Note that, $\tilde{G}$ is a two-dimensional mixed discrete and continuous random field (discrete over components and continuous over time).

In terms of notation, the system response can be modeled as a two-dimensional random field $\tilde{G}(\mathbf{d}, \theta)$, where θ represents the randomness of the random field and $\mathbf{d}$ is the vector of coordinates, denoted as $\mathbf{d} = [i, t]$, where i is the component index and t is time.

3.3 Modeling of System Random Field Response. Since the limit-state functions $G_i(t) = g_i(\mathbf{X}, \mathbf{Y}(t), t)$, $i = 1, 2, \cdots, n$ are usually nonlinear functions of random variables $\mathbf{X}$, stochastic processes $\mathbf{Y}(t)$, and time t, $\tilde{G}(\mathbf{d}, \theta)$ is in general a non-Gaussian nonstationary random field. Directly modeling this two-dimensional random field is difficult. However, a general non-Gaussian random field $\tilde{G}(\mathbf{d}, \theta)$ can be mapped into an equivalent Gaussian random field, $L(\mathbf{d}, \theta)$, as below:

$$L(\mathbf{d}, \theta) = \Phi^{-1}\left[F_{\tilde{G}}(\tilde{G}(\mathbf{d}, \theta))\right] \tag{9}$$

where $\Phi^{-1}[\cdot]$ is the inverse cumulative density function (CDF) of a standard normal variable and $F_{\tilde{G}}(\cdot)$ is the CDF of random field $\tilde{G}(\mathbf{d}, \theta)$ at point $\mathbf{d}$.

The above equation is for a random field with known statistical information. In time-dependent system reliability analysis, however, the statistical information on $\tilde{G}(\mathbf{d}, \theta)$ is not explicit. It is governed by $G_i(t) = g_i(\mathbf{X}, \mathbf{Y}(t), t)$, $i = 1, 2, \cdots, n$. To make the modeling of $\tilde{G}(\mathbf{d}, \theta)$ possible, we map the non-Gaussian random field $\tilde{G}(\mathbf{d}, \theta)$ into an equivalent Gaussian random field $L(\mathbf{d}, \theta)$ based on the following probability equivalency:

$$\Pr\{\tilde{G}(\mathbf{d}, \theta) > 0\} \approx \Pr\{L(\mathbf{d}, \theta) > 0\} \tag{10}$$

In this paper, the mapping from $\tilde{G}(\mathbf{d}, \theta)$ to $L(\mathbf{d}, \theta)$ is achieved through the use of the FORM.

3.3.1 Mapping $\tilde{G}(\mathbf{d}, \theta)$ to $L(\mathbf{d}, \theta)$. Recall that for a given point $\mathbf{d}_1 = [i, t_1]$ in the two-dimensional domain of $\tilde{G}(\mathbf{d}, \theta)$, the corresponding non-Gaussian random response $\tilde{G}(\mathbf{d}_1, \theta)$ is given by $\tilde{G}(\mathbf{d}_1, \theta) = g_i(\mathbf{X}, \mathbf{Y}(t_1), t_1)$. In order to transform $\tilde{G}(\mathbf{d}_1, \theta)$ into $L(\mathbf{d}_1, \theta)$ as indicated in Eq. (10), the most probable point (MPP) of $\Pr\{\tilde{G}(\mathbf{d}_1, \theta) = g_i(\mathbf{X}, \mathbf{Y}(t_1), t_1) > 0\}$ is first estimated by solving the following optimization:

$$\begin{cases} \min\limits_{\mathbf{u}} \|\mathbf{u}\| \\ g_i(T(\mathbf{u}), t_1) \le 0 \end{cases} \tag{11}$$

where $T(\cdot)$ stands for an operator that transforms Gaussian random variables $\mathbf{U} = [\mathbf{U}_X, \mathbf{U}_Y(t_1)]$ to original random variables, $\mathbf{X}$ and $\mathbf{Y}(t_1)$, and $\mathbf{u} = [\mathbf{u}_X, \mathbf{u}_Y(t_1)]$ is a realization of $\mathbf{U} = [\mathbf{U}_X, \mathbf{U}_Y(t_1)]$.

At the obtained MPP, $\mathbf{u}^*(\mathbf{d}_1) = [\mathbf{u}_X^*, \mathbf{u}_Y^*]$, we have the following probability equivalency:

$$\Pr\{\tilde{G}(\mathbf{d}_1, \theta) = g_i(\mathbf{X}, \mathbf{Y}(t_1), t_1) > 0\} \approx \Pr\{\boldsymbol{\alpha}(\mathbf{d}_1)\mathbf{U}^{\mathrm{T}} - \beta(\mathbf{d}_1) > 0\} \tag{12}$$

where $\boldsymbol{\alpha}(\mathbf{d}_1) = -\mathbf{u}^*(\mathbf{d}_1)/\|\mathbf{u}^*(\mathbf{d}_1)\|$ and $\beta(\mathbf{d}_1) = \|\mathbf{u}^*(\mathbf{d}_1)\|$.

Thus for any given point $\mathbf{d}_1$ in the domain of $\tilde{G}(\mathbf{d}, \theta)$, $\tilde{G}(\mathbf{d}_1, \theta)$ can be mapped into a Gaussian response $L(\mathbf{d}_1, \theta) = \boldsymbol{\alpha}(\mathbf{d}_1)\mathbf{U}^{\mathrm{T}} - \beta(\mathbf{d}_1)$ using FORM. If the FORM is performed at every point of $\tilde{G}(\mathbf{d}, \theta)$, $\tilde{G}(\mathbf{d}, \theta)$ can be mapped into the equivalent Gaussian random field $L(\mathbf{d}, \theta)$. Performing FORM at every point, however, is computationally very expensive. To reduce the computational cost, we model the equivalent Gaussian random field $L(\mathbf{d}, \theta)$ by following the approach presented in Ref. [13].

3.3.2 Modeling of the Equivalent Random Field. $L(\mathbf{d}, \theta)$ is a Gaussian random field. During the past several decades, many approaches have been proposed for the modeling of Gaussian random fields, such as Karhunen–Loève (KL) and polynomial chaos expansions (PCE), the shape function method [23], optimal linear estimation, expansion optimal linear estimation (EOLE) [23], and proper orthogonal decomposition [24]. A review about the modeling of Gaussian random fields is available in Ref. [23]. Among these methods, the dominant approach to model the random field using its important features is as follows:

$$L(\mathbf{d}, \theta) \approx \mu_L(\mathbf{d}) + \sigma_L(\mathbf{d}) \sum_{i=1}^{r} \xi_i(\theta)\boldsymbol{\gamma}_i(\mathbf{d}) \tag{13}$$

where $\mu_L(\mathbf{d})$ is the mean value function of the random field $L(\mathbf{d}, \theta)$, $\sigma_L(\mathbf{d})$ is the standard deviation of $L(\mathbf{d}, \theta)$, ξ_i, $i = 1, 2, \cdots, r$ are independent random variables, $\boldsymbol{\gamma}_i(\mathbf{d})$ is the ith important feature, and r is the number of important features used to model the random field. Each realization of $\xi_i(\theta)$, $i = 1, 2, \cdots, r$, gives a realization of the random field. The number of important features is determined according to the magnitude of the eigenvalues obtained from the covariance matrix as given in Eq. (14).

In order to obtain the important features of the random field $L(\mathbf{d}, \theta)$, the EOLE method is employed in this paper since it is more efficient than the KL expansion method. In the EOLE method, the domain of the random field is first discretized. Since the random field $G(\mathbf{d}, \theta)$ is a mixed discrete and continuous random field, $L(\mathbf{d}, \theta)$ is a mixed random field as well. In order to implement the EOLE method, we discretize the continuous dimension (time) into s points. After combining the s points of time with the discrete component indices, we have $n \times s$ points in the domain of $L(\mathbf{d}, \theta)$, where n is the number of components. Denoting these points as $\mathbf{d}_1, \cdots, \mathbf{d}_{ns}$, we have the following correlation matrix:

$$\Sigma = \begin{pmatrix} \rho_L(\mathbf{d}_1, \mathbf{d}_1) & \rho_L(\mathbf{d}_1, \mathbf{d}_2) & \cdots & \rho_L(\mathbf{d}_1, \mathbf{d}_{ns}) \\ \rho_L(\mathbf{d}_2, \mathbf{d}_1) & \rho_L(\mathbf{d}_2, \mathbf{d}_2) & \cdots & \rho_L(\mathbf{d}_2, \mathbf{d}_{ns}) \\ \vdots & \vdots & \ddots & \vdots \\ \rho_L(\mathbf{d}_{ns}, \mathbf{d}_1) & \rho_L(\mathbf{d}_{ns}, \mathbf{d}_2) & \cdots & \rho_L(\mathbf{d}_{ns}, \mathbf{d}_{ns}) \end{pmatrix}_{ns \times ns} \tag{14}$$

in which $\rho_L(\mathbf{d}_i, \mathbf{d}_j)$ is the correlation between two points $\mathbf{d}_i$ and $\mathbf{d}_j$ in the domain of $L(\mathbf{d}, \theta)$.

We then perform eigenvalue and eigenvector analysis for the correlation matrix. Let $\boldsymbol{\eta} = [\eta_1, \eta_2, \ldots, \eta_{ns}]$ be the obtained eigenvalues and $\boldsymbol{\phi}_1, \boldsymbol{\phi}_2, \ldots, \boldsymbol{\phi}_{ns}$ be the associated eigenvectors, we then rank the eigenvalues and eigenvectors according to the magnitude of eigenvalues [25]. According to the rank of eigenvalues, we select the first r largest eigenvalues and corresponding eigenvectors to construct important features for $L(\mathbf{d}, \theta)$. In the EOLE method, the important feature $\boldsymbol{\gamma}_i(\mathbf{d})$ is given as a function of eigenvalue and eigenvector as follows:

$$\boldsymbol{\gamma}_i(\mathbf{d}) = \boldsymbol{\phi}_i^{\mathrm{T}}\boldsymbol{\rho}_L(\mathbf{d})/\sqrt{\eta_i} \tag{15}$$

where $\boldsymbol{\rho}_L(\mathbf{d}) = [\rho_L(\mathbf{d}, \mathbf{d}_1), \rho_L(\mathbf{d}, \mathbf{d}_2), \ldots, \rho_L(\mathbf{d}, \mathbf{d}_{ns})]^{\mathrm{T}}$.

The Gaussian random field $L(\mathbf{d}, \theta)$ is then represented as [13]

$$L(\mathbf{d}, \theta) \approx \mu_L(\mathbf{d}) + \sigma_L(\mathbf{d}) \sum_{i=1}^{r} \xi_i(\theta)\gamma_i(\mathbf{d}) = \mu_L(\mathbf{d}) + \sigma_L(\mathbf{d}) \sum_{i=1}^{r} \xi_i(\theta)(\boldsymbol{\phi}_i^{\mathrm{T}} \boldsymbol{\rho}_L(\mathbf{d})/\sqrt{\eta_i}) \tag{16}$$

in which $\mathbf{d} = [j, t], j \in \{1, 2, \cdots, n\}$, and $t \in [t_0, t_e]$. In the above equation, ξ_i, $i = 1, 2, \cdots, r$ are independent standard normal variables.

In the above modeling process of the equivalent random field $L(\mathbf{d}, \theta)$, the mean, standard deviation, and the correlation functions are required. From the property of FORM, the mean and standard deviation of $L(\mathbf{d}, \theta)$ are given as

$$\mu_{L(\mathbf{d},\theta)} = -\beta(\mathbf{d}) \tag{17}$$

$$\sigma_{L(\mathbf{d}_1,\theta)} = 1 \tag{18}$$

where $\beta(\mathbf{d})$ is the reliability index obtained from MPP at point $\mathbf{d}$.

The correlation $\rho_L(\mathbf{d}_i, \mathbf{d}_j)$ between any two points $\mathbf{d}_i$ and $\mathbf{d}_j$ of the $L(\mathbf{d}, \theta)$ is given by

$$\rho_L(\mathbf{d}_i, \mathbf{d}_j) = \boldsymbol{\alpha}_{\mathbf{X}}(\mathbf{d}_i)\boldsymbol{\alpha}_{\mathbf{X}}^{\mathrm{T}}(\mathbf{d}_j) + \boldsymbol{\alpha}_{\mathbf{Y}}(\mathbf{d}_i)\boldsymbol{\rho}_Y(t_i, t_j)\boldsymbol{\alpha}_{\mathbf{Y}}^{\mathrm{T}}(\mathbf{d}_j) \tag{19}$$

where $\boldsymbol{\alpha}_{\mathbf{X}}(\mathbf{d}_i) = -\mathbf{u}_X^*(\mathbf{d}_i)/\|\mathbf{u}^*(\mathbf{d}_i)\|$, $\boldsymbol{\alpha}_{\mathbf{X}}(\mathbf{d}_j) = -\mathbf{u}_X^*(\mathbf{d}_j)/\|\mathbf{u}^*(\mathbf{d}_j)\|$, $\boldsymbol{\alpha}_{\mathbf{Y}}(\mathbf{d}_i) = -\mathbf{u}_Y^*(\mathbf{d}_i)/\|\mathbf{u}^*(\mathbf{d}_i)\|$, $\boldsymbol{\alpha}_{\mathbf{Y}}(\mathbf{d}_j) = -\mathbf{u}_Y^*(\mathbf{d}_j)/\|\mathbf{u}^*(\mathbf{d}_j)\|$, $\mathbf{u}^*(\mathbf{d}_i)$, and $\mathbf{u}^*(\mathbf{d}_j)$ are MPPs obtained from MPP search at points $\mathbf{d}_i$ and $\mathbf{d}_j$, and $\boldsymbol{\rho}_Y(t_i,t_j)$ is given by

$$\boldsymbol{\rho}_Y(t_i, t_j) = \begin{bmatrix} \rho_{Y_1}(t_i, t_j) & 0 & \cdots & 0 \\ 0 & \ddots & \cdots & 0 \\ \vdots & \vdots & \ddots & \vdots \\ 0 & 0 & \cdots & \rho_{Y_{m2}}(t_i, t_j) \end{bmatrix}_{m2\times m2} \tag{20}$$

in which $m2$ is the number of stochastic processes in the system inputs and $\rho_{Y_i}(t_1, t_2)$ is the correlation function of stochastic process $Y_i(t)$.

During the modeling of $L(\mathbf{d}, \theta)$, Eqs. (17)–(20) repeatedly evaluated the limit-state functions. The computational effort is still very intensive. In order to reduce the number of function evaluations in the limit-state functions, we construct surrogate models for $\mu_L(\mathbf{d}) = -\beta(\mathbf{d})$ and $\rho_L(\mathbf{d}_i, \mathbf{d}_j)$.

3.3.3 Surrogate Models of $\beta(\mathbf{d})$ and $\rho_L(\mathbf{d}_i, \mathbf{d}_j)$. There are many surrogate model methods available, such as PCE method, support vector machine, and kriging [26]. Since the input variables $\mathbf{d}$ are mixed discrete and continuous variables with component index being discrete and time being continuous, the surrogate model employed must be able to accommodate these two kinds of variables. Swiler et al. studied the surrogate model approaches for mixed discrete-continuous variables [27]. Results from their test problems indicate that the adaptive component selection and shrinkage operator method and the kriging model with special correlation functions generally performed well and the latter is the most consistent [27]. In this paper, we therefore use the kriging model with spatial correlation functions to construct the surrogate model for $\beta(\mathbf{d})$ and $\rho_L(\mathbf{d}_i, \mathbf{d}_j)$. The developed method, however, is not limited to the kriging model.

(a) *Design of experiments*: In order to generate the training points for surrogate models, we first uniformly discretize the time interval $[t_0, t_e]$ into nt points. Combining the nt time points with the component index, we have the following training points

$$\mathbf{d}^t_{(i-1)nt+j} = [i, t_j] \tag{21}$$

where $\mathbf{d}^t_{(i-1)nt+j}$ stands for the $(i-1)nt+j$th training point, where $i = 1, 2, \cdots, n$ and $t_j = t_0 + j[(t_e - t_0)/nt], j = 1, 2, \cdots, nt$. Note that the superscript "t" indicates training points, not transpose.

For each training point $\mathbf{d}^t_{(i-1)nt+j}$, an MPP search is performed using the following equation:

$$\begin{cases} \min\limits_{\mathbf{u}} \|\mathbf{u}\| \\ g_i(T(\mathbf{u}), t_j) \le 0 \end{cases} \tag{22}$$

It should be noted that $G_i = g_i(T(\mathbf{u}), t_j)$ is the limit-state function of component i. From the $n \times nt$ MPP searches, we obtain $\boldsymbol{\beta}^t = [\beta(\mathbf{d}^t_1), \beta(\mathbf{d}^t_2), \cdots, \beta(\mathbf{d}^t_{n\times nt})]$ and $\boldsymbol{\alpha}^t = [\boldsymbol{\alpha}(\mathbf{d}^t_1), \boldsymbol{\alpha}(\mathbf{d}^t_2), \cdots, \boldsymbol{\alpha}(\mathbf{d}^t_{n\times nt})]$.

(b) *Surrogate models of $\beta(\mathbf{d})$ and $\rho_L(\mathbf{d}_i, \mathbf{d}_j)$* : With the training points $\mathbf{d}^t$ and the corresponding reliability indices $\boldsymbol{\beta}^t$, a surrogate model can be constructed for $\beta(\mathbf{d})$ using the kriging approach. Details about the kriging model method are available in Ref. [26]. Constructing the surrogate model for $\rho_L(\mathbf{d}_i, \mathbf{d}_j)$ is different from that for $\beta(\mathbf{d})$. This is a four-dimensional surrogate model with symmetric geometry. From the design of experiments, we have training points of $\mathbf{d}^t$ and $\boldsymbol{\alpha}^t$. These training points, however, cannot be applied to the surrogate modeling of $\rho_L(\mathbf{d}_i, \mathbf{d}_j)$ directly. The training points of $\rho_L(\mathbf{d}_i, \mathbf{d}_j)$ are obtained by combining all points in $\mathbf{d}^t$; we therefore have

$$\mathbf{dd}^t = [\mathbf{d}^t_k, \mathbf{d}^t_l], \forall k, l = 1, 2, \cdots, n \times nt \tag{23}$$

For each element of $\mathbf{dd}^t = [\mathbf{d}^t_k, \mathbf{d}^t_l]$, the corresponding correlation $\rho_L(\mathbf{d}^t_k, \mathbf{d}^t_l)$ is computed using Eq. (19) by substituting $\boldsymbol{\alpha}(\mathbf{d}^t_k)$ and $\boldsymbol{\alpha}(\mathbf{d}^t_l)$ into the equation.

Since $\rho_L(\mathbf{d}_i, \mathbf{d}_i) = 1$ for any point $\mathbf{d}_i$ in the domain of the surrogate model $\rho_L(\mathbf{d}_i, \mathbf{d}_j)$, we can add extra training points along the line $\mathbf{d}_i = \mathbf{d}_i$ of the surrogate model without calling the limit-state functions. Based on the training points $\mathbf{dd}^t = [\mathbf{d}^t_k, \mathbf{d}^t_l]$ and $\boldsymbol{\rho}^t = \rho_L(\mathbf{d}^t_k, \mathbf{d}^t_l), \forall k, l = 1, 2, \cdots, n \times nt$, the surrogate model $\hat{\rho}_L(\mathbf{d}_i, \mathbf{d}_j)$ is constructed using the kriging approach.

(c) *Flowchart of constructing the surrogate model*: After the surrogate models of $\hat{\beta}(\mathbf{d})$ and $\hat{\rho}_L(\mathbf{d}_i, \mathbf{d}_j)$ are constructed, the accuracies of the surrogate models are verified by analyzing the maximum mean square errors (MSE) of the surrogate models. Figure 2 shows a brief flowchart for the surrogate modeling of $\hat{\beta}(\mathbf{d})$ and $\hat{\rho}_L(\mathbf{d}_i, \mathbf{d}_j)$.

Based on the surrogate models of $\hat{\beta}(\mathbf{d})$ and $\hat{\rho}_L(\mathbf{d}_i, \mathbf{d}_j)$, the equivalent random field $L(\mathbf{d}, \theta)$ is modeled using Eqs. (13)–(16). Next, we discuss how to perform time-dependent system reliability analysis based on logistical analysis on the equivalent random field.

3.4 Reliability Analysis Based on System Topology

3.4.1 Discretization of Equivalent Random Field $L(\mathbf{d}, \theta)$. Even though the equivalent random field $L(\mathbf{d}, \theta)$ is presented as a combination of important features as given in Eq. (16), there is no analytical solution available for the global extreme value distributions of the nonstationary Gaussian random field. To perform time-dependent system reliability analysis, we rely on the simulation method by discretizing the equivalent random field. The time

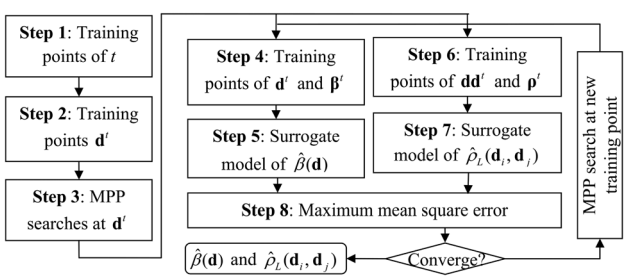

Fig. 2 Flowchart for surrogate modeling of $\hat{\beta}(\mathbf{d})$ and $\hat{\rho}_L(\mathbf{d}_i, \mathbf{d}_j)$

interval $[t_0, t_e]$ is discretized into q time instants with $t_i = t_0 + i(t_e - t_0)/q$, $i = 1, 2, \ldots, q$. The q time instants are then combined with the n-component indexes to formulate discrete points in the domain of $L(\mathbf{d}, \theta)$. From the combinations, we have $\mathbf{d}_{(i-1)q+j} = [i, t_j]$, where $i = 1, 2, \ldots, n$ and $j = 1, 2, \ldots, q$. Assume that we generate n_{MCS} samples for the standard normal variables ξ_i, $i = 1, 2, \ldots, r$, n_{MCS} realizations of the random field are obtained. Based on Eq. (16), $\hat{\beta}(\mathbf{d})$ and $\hat{\rho}_L(\mathbf{d}_1, \mathbf{d}_2)$, and the eigenvalue analysis given in Sec. 3.3.2, we obtain a two-dimensional sample matrix for $L(\mathbf{d}, \theta)$ as follows:

$$L_{n_{\text{MCS}} \times nq} = \begin{bmatrix} L(\mathbf{d}_1, 1) & L(\mathbf{d}_2, 1) & \cdots & L(\mathbf{d}_{nq}, 1) \\ L(\mathbf{d}_1, 2) & L(\mathbf{d}_2, 2) & \cdots & L(\mathbf{d}_{nq}, 2) \\ \vdots & \vdots & \ddots & \vdots \\ L(\mathbf{d}_1, n_{\text{MCS}}) & L(\mathbf{d}_2, n_{\text{MCS}}) & \cdots & L(\mathbf{d}_{nq}, n_{\text{MCS}}) \end{bmatrix}_{n_{\text{MCS}} \times nq} \tag{24}$$

in which $L(\mathbf{d}_i, j)$ is the jth realization of the random field at point $\mathbf{d}_i$ and $L(\mathbf{d}_i, j)$, $i = 1, 2, \cdots, nq$ is the jth realization of the random field. Since the discretization will not evaluate the original limit-state function, an appropriate number of discretization points can be determined by checking the convergence of reliability analysis results.

3.4.2 Time-Dependent System Probability of Failure and Failure Sequence Analyses. To perform time-dependent system probability of failure analysis, we first define the following logical (failure) indicator:

$$F(i, j) = \begin{cases} 1, L(\mathbf{d}_i, j) > 0 \\ 0, L(\mathbf{d}_i, j) \le 0 \end{cases} \tag{25}$$

Since $\mathbf{d}_{(i-1)q+j} = [i, t_j]$, realizations from $L(\mathbf{d}_{(i-1)q+1}, k)$ to $L(\mathbf{d}_{(i-1)q+q}, k)$ correspond to the kth realization of component i over the time interval $[t_0, t_e]$. The time-dependent probability of failure for component i (Eq. (4)) is therefore given by

$$p_f^i(t_0, t_e) = \sum_{k=1}^{n_{\text{MCS}}} \max_{j=1,\cdots,q} (F((i-1)q + j, k))/n_{\text{MCS}} \tag{26}$$

We also define a component failure indicator as follows:

$$I_i(k) = \begin{cases} 1, G_i(t) = g_i(\mathbf{x}, \mathbf{y}(t), t) > 0, \exists t \in [t_0, t_e] \\ 0, G_i(t) = g_i(\mathbf{x}, \mathbf{y}(t), t) \le 0, \forall t \in [t_0, t_e] \end{cases} \tag{27}$$

where $\mathbf{x}$ is a realization of $\mathbf{X}$, $\mathbf{y}(t)$ is a realization of $\mathbf{Y}(t)$, $I_i(k) = 1$ indicates that the realization of the response of component i is failed over the time period $[t_0, t_e]$, and $I_i(k) = 0$ indicates that the component is safe.

Since the failure event $G_i(t) = g_i(\mathbf{X}, \mathbf{Y}(t), t) > 0$ is equivalent to the failure event $L(\mathbf{d}, \theta) = \boldsymbol{\alpha}(\mathbf{d})\mathbf{U}^{\mathrm{T}} - \beta(\mathbf{d}) > 0$, $\mathbf{d} = [i, t]$, we have

$$I_i(k) = \max_{j=1,\cdots,q} (F((i-1)q + j, k)) \tag{28}$$

Based on the component safety indicator, Boolean functions are defined for series and parallel systems. The defined functions are given by

$$\begin{aligned} I_s(k) = \{&G_i(t_i) = g_i(\mathbf{x}, \mathbf{y}(t_i), t_i) > 0, \quad \exists t_i \in [t_0, t_e] \\ \cup &G_j(t_j) = g_j(\mathbf{x}, \mathbf{y}(t_j), t_j) > 0, \quad \exists t_j \in [t_0, t_e]\} = I_i(k) + I_j(k) \end{aligned} \tag{29}$$

$$\begin{aligned} I_s(k) = \{&G_i(t_i) = g_i(\mathbf{x}, \mathbf{y}(t_i), t_i) > 0, \quad \exists t_i \in [t_0, t_e] \\ \cap &G_j(t_j) = g_j(\mathbf{x}, \mathbf{y}(t_j), t_j) > 0, \quad \exists t_j \in [t_0, t_e]\} = I_i(k) I_j(k) \end{aligned} \tag{30}$$

where $I_s(k)$ is the system failure indicator for the kth realization of the system with $I_s(k) > 0$ is failed and $I_s(k) = 0$ is safe.

Applying the defined indicators and Boolean functions to the time-dependent system probability of failure given in Eqs. (5) and (6), we then have

$$p_f^{\text{system}} = \sum_{k=1}^{n_{\text{MCS}}} I_r(k)/n_{\text{MCS}} \tag{31}$$

where $I_r(k) = 1$ if $I_s(k) > 0$, otherwise $I_r(k) = 0$. For the series system, $I_s(k) = \sum_{i=1}^{n} I_i(k)$. For the parallel system, $I_s(k) = \prod_{i=1}^{n} I_i(k)$. For the combined and linked network systems, $I_s(k)$ is defined according to the system topology. For example, for a Wheatstone bridge system as given in Fig. 3, binary decomposition needs to be performed first. Based on this, the original linked network system is transformed into combined systems [28]. With the Boolean function defined according to the system topology and Eq. (28), the system reliability is estimated using Eq. (31). Since the computer simulations and system response modeling are independent from the system topology (Boolean function) in the developed method (as indicated in Fig. 1), the application of the developed method is not limited by the topology of the system.

Based on the sampling matrix given in Eq. (24) and the failure indicators, the important failure sequences can also be obtained. Since it is a byproduct of the system reliability analysis and is quite straightforward based on the sampling matrix, we do not provide algorithmic details for failure sequence analysis.

3.5 Implementation. This section summarizes the general procedure for the time-dependent system reliability analysis method based on the random field discretization. There are mainly six steps:

Step 1: Generate uniformly spaced training points of t over the time interval of interest.
Step 2: Construct surrogate models for $\hat{\beta}(\mathbf{d})$ and $\hat{\rho}_L(\mathbf{d}_1, \mathbf{d}_2)$ according to the procedure presented in Sec. 3.3.3.
Step 3: Perform eigenvalue and eigenvector analysis for the correlation matrix given in Eq. (14).
Step 4: Select the eigenvectors corresponding to the r largest eigenvalues to model the equivalent random field.
Step 5: Discretize the obtained equivalent random field and generate samples using MCS for the random field.
Step 6: Perform time-dependent component reliability analysis, system reliability analysis, and failure sequence analysis based on the generated samples.

4 Error Analysis

Three main approximations are made in the proposed approach: (1) linearization of the limit state in FORM, (2) expansion of Gaussian random field using important features, and (3) surrogate models for mean and correlation function of the equivalent random field. The effects of these approximations on the reliability analysis results are problem-dependent, affected by the system behavior (e.g., linear versus nonlinear), available data (for random field modeling), and computational resources (for surrogate model training). The error in the reliability analysis result mainly comes from the FORM approximation and surrogate model error. As

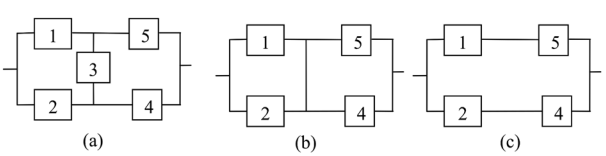

Fig. 3 An example of a network system: (*a*) Wheatstone bridge system, (*b*) $I_3 = 1$, and (*c*) $I_3 = 0$

mentioned in Sec. 2.2, the developed method is applicable for problems where the FORM is accurate for time-instantaneous reliability analysis. Here, we therefore mainly focus on quantifying the uncertainty in time-dependent reliability analysis results due to the uncertainty of surrogate models of $\hat{\beta}(\mathbf{d})$ and $\hat{\rho}_L(\mathbf{d}_1, \mathbf{d}_2)$. The main idea of the error analysis is to propagate the uncertainty in $\hat{\beta}(\mathbf{d})$ and $\hat{\rho}_L(\mathbf{d}_1, \mathbf{d}_2)$ through the time-dependent reliability analysis presented in Sec. 3.3. Samples of $\hat{\beta}(\mathbf{d})$ and $\hat{\rho}_L(\mathbf{d}_1, \mathbf{d}_2)$ are generated first. The generated samples are then propagated through the time-dependent reliability analysis framework (Secs. 3.3 and 3.4) to get the samples of time-dependent reliability analysis results. Based on this, the prediction intervals of the analysis results are obtained.

Note that the above error analysis will not evaluate the original limit-state functions. Only the surrogate models of $\hat{\beta}(\mathbf{d})$ and $\hat{\rho}_L(\mathbf{d}_1, \mathbf{d}_2)$ will be evaluated.

5 Numerical Examples

In this section, three examples: a series system, a parallel system, and a combined system are used to demonstrate the effectiveness of the proposed method.

5.1 Series System: A Function Generator Mechanism. Figure 4 shows a function generator mechanism [29]. This system consists of two four-bar linkage mechanisms, which are used to generate a sine and a logarithm function, respectively.

For mechanism 1 (the sine function generator), the motion input and output are θ and $\kappa = \kappa_a(\mathbf{B}, \theta)$, respectively, where $\mathbf{B} = [B_1, B_2, \ldots, B_7]$ are the lengths of linkages of the mechanism. The required motion output is given by

$$\kappa_d(\theta) = 60\,\text{deg} + 60\,\text{deg}\,\sin[0.75(\theta - 97\,\text{deg})] \tag{32}$$

For mechanism 2 (the logarithm function generator), the motion input and output are χ and $\eta = \eta_a(\mathbf{B}, \chi)$, respectively. The required motion output is

$$\eta_d(\chi) = 60\,\text{deg}\log_{10}[(\chi + 15\,\text{deg})/60\,\text{deg}]/\log_{10}(2) \tag{33}$$

The motion errors of the two mechanisms are given by

$$\varepsilon_\kappa(\mathbf{B}, \theta) = \kappa_a(\mathbf{B}, \theta) - \kappa_d(\theta) \tag{34}$$

$$\varepsilon_\eta(\mathbf{B}, \chi) = \eta_a(\mathbf{B}, \chi) - \eta_d(\chi) \tag{35}$$

Links B_2 and B_5 are welded together, and the two input angles satisfy

$$\theta = 62\,\text{deg} + \chi \tag{36}$$

From the mechanism analysis, the following equations can be obtained:

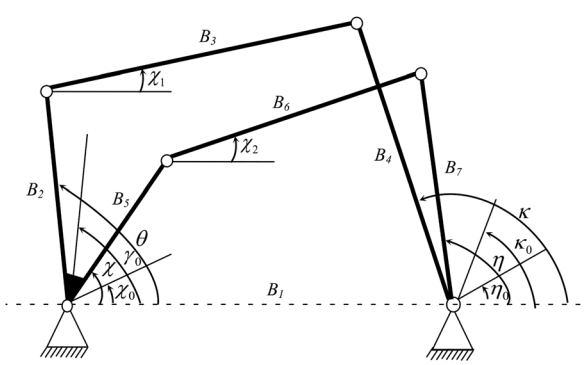

Fig. 4 A function generator mechanism system

$$\kappa_a(\mathbf{B}, \theta) = 2\arctan\left(\left(-E_\kappa \pm \sqrt{E_\kappa^2 + D_\kappa^2 - F_\kappa^2}\right)/(F_\kappa - D_\kappa)\right) \tag{37}$$

where $D_\kappa = 2B_4(B_1 - B_2\cos\theta)$, $E_\kappa = -2B_2B_4\sin\theta$, and $F_\kappa = B_1^2 + B_2^2 + B_4^2 - B_3^2 - 2B_1B_2\cos\theta$.

$$\eta_a(\mathbf{B}, \chi) = 2\arctan\left(\left(-E_\eta \pm \sqrt{E_\eta^2 + D_\eta^2 - F_\eta^2}\right)/(F_\eta - D_\eta)\right) \tag{38}$$

$$\eta_d(\chi) = 60\,\text{deg}\log_{10}[(\chi + 15\,\text{deg})/60\,\text{deg}]/\log_{10}(2) \tag{39}$$

where $D_\eta = 2B_7(B_1 - B_5\cos\chi)$, $E_\eta = -2B_5B_7\sin\chi$, and $F_\eta = B_1^2 + B_5^2 + B_7^2 - B_6^2 - 2B_1B_5\cos\chi$.

In this problem, there is no stochastic process in the input variables and the time varying factor is χ. Since the statistical properties of both of the motion errors change with time, the motion errors responses are still stochastic processes. We would like the mechanism system to perform its intended functions over $[\chi_0, \chi_s] = [45\,\text{deg}, 105\,\text{deg}]$. If any motion error is greater than its allowable value over the angle interval of interest, the system is considered to be failed. The system is therefore a series system and the system probability of failure is given by

$$p_f^{\text{system}}(\chi_0, \chi_s) = \Pr\{\varepsilon_\kappa(\mathbf{B}, \chi_i) - e_1 > 0 \cup \varepsilon_\eta(\mathbf{B}, \chi_j) - e_2 > 0, \exists \chi_i, \chi_j \in [\chi_0, \chi_s]\} \tag{40}$$

where $e_1 = 1.4\,\text{deg}$ and $e_2 = 1.4\,\text{deg}$ are the allowable motion errors. Table 1 gives the parameters of example 1.

We perform time-dependent system reliability analysis using the proposed method and a basic MCS implementation. In MCS, the time interval is discretized into 200 time instants and 1×10^6 samples are generated at each time instant. Since there are two limit-state functions, the total number of function evaluations in MCS is 4×10^8. In the proposed method, the input angle interval $[45\,\text{deg}, 105\,\text{deg}]$ is divided into 15 time instants. The MPP searches are performed 30 times to construct the surrogate models for $\hat{\beta}(\mathbf{d})$ and $\hat{\rho}_L(\mathbf{d}_i, \mathbf{d}_j)$. The total number of function evaluations for the proposed method is **1,112**.

Based on the eigenvalue and eigenvector analysis, the first five important features are used to model the equivalent random field $L(\mathbf{d}, \theta)$. By performing sampling on the constructed equivalent random field, the time-dependent component probability of failure, system probability of failure, and the failure sequences are analyzed using the formulas given in Sec. 3.4. Figures 5(*a*)–5(*c*) show the comparison of time-dependent component probability of failure and system probability of failure obtained from the proposed method and MCS. The 95% prediction intervals of the proposed method due to the surrogate model uncertainty are also given in Fig. 5. Table 2 gives the percentage error of reliability analysis results over the time interval of interest. The results show that the proposed method is able to accurately approximate both component and system time-dependent probabilities of failure. We also perform failure sequence analysis for this example. Since it is a series system with two components, there are only two failure sequences: component one fails first (sequence 1) and component 2 fails first (sequence 2). Figure 5(*d*) gives the failure

Table 1 Parameters in example 1

	B_1 (mm)	B_2 (mm)	B_3 (mm)	B_4 (mm)	B_5 (mm)	B_6 (mm)	B_7 (mm)
Mean	100	55.5	144.1	72.5	79.5	203	150.8
Std.	0.3	0.05	0.05	0.05	0.05	0.05	0.05
Dist.	Normal	Normal	Normal	Normal	Normal	Normal	Normal

Note: "Std." stands for standard deviation and "Dist." for distribution.

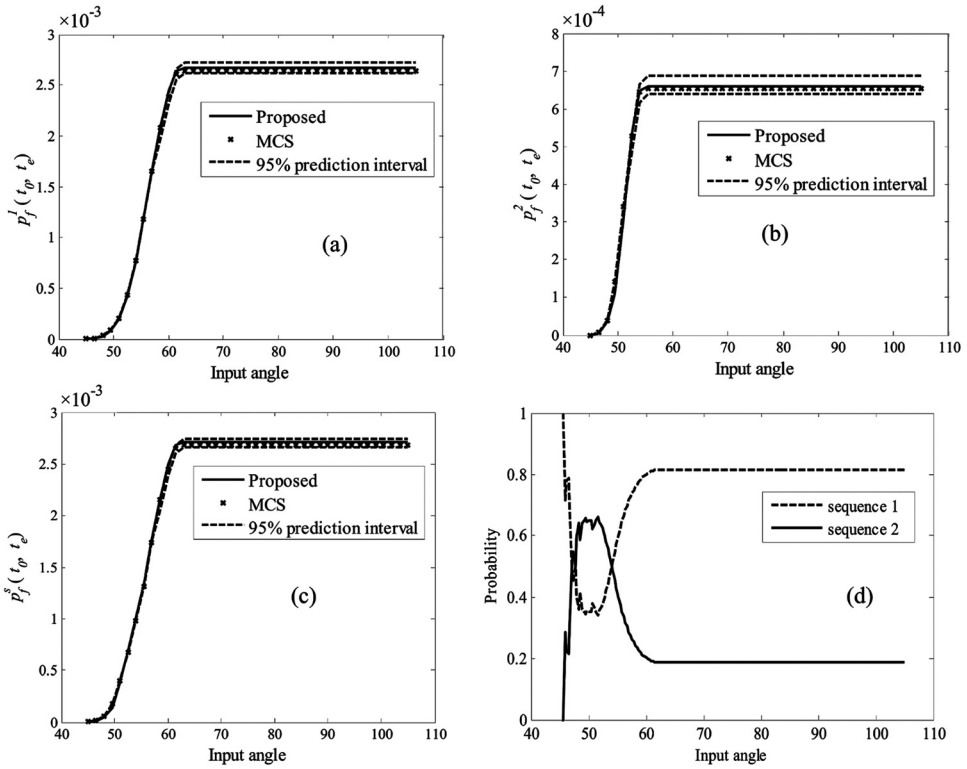

Fig. 5 Time-dependent system probability of failure and failure sequences: (*a*) component 1, (*b*) component 2, (*c*) system, and (*d*) failure sequences

Table 2 Percentage error of the proposed method for the three numerical examples

					Percentage error of example 1						
TI (deg)		[45, 48]	[45, 51]	[45, 54]	[45, 57]	[45, 60]	[45, 70]	[45, 80]	[45, 90]	[45, 100]	[45, 105]
$\varepsilon(\%)$	C1	1.00	4.97	4.50	1.67	0.86	0.86	0.86	0.86	0.86	0.86
	C2	6.77	1.07	1.06	1.06	1.06	1.06	1.06	1.06	1.06	1.06
	S	4.26	3.92	4.04	1.64	0.66	0.66	0.66	0.66	0.66	0.66
					Percentage error of example 2						
TI (yr)		[0, 1]	[0, 2]	[0, 3]	[0, 4]	[0, 5]	[0, 6]	[0, 7]	[0, 8]	[0, 9]	[0, 10]
$\varepsilon(\%)$	C1	4.16	0.05	0.53	1.27	0.91	0.99	1.51	1.76	1.28	0.74
	C2	2.02	1.35	1.58	1.73	1.54	1.29	1.94	2.07	1.83	1.37
	S	2.47	0.74	0.71	1.55	0.22	0.22	0.69	0.26	0.35	1.87
					Percentage error of example 3						
TI (years)		[0, 1]	[0, 2]	[0, 3]	[0, 4]	[0, 5]	[0, 6]	[0, 7]	[0, 8]	[0, 9]	[0, 10]
$\varepsilon(\%)$	C1	1.06	0.85	1.12	0.66	0.61	1.03	0.97	0.80	0.83	1.00
	C2	2.98	1.74	1.60	1.49	1.50	1.66	1.55	1.48	1.67	1.55
	C3	7.63	9.26	6.93	7.70	1.75	1.04	0.81	1.54	3.67	3.53
	C4	0.87	0.57	1.88	4.36	1.82	2.03	0.42	0.38	0.95	3.11
	C5	8.10	6.39	4.85	8.57	9.54	7.96	6.43	4.74	3.41	1.83
	C6	1.75	4.90	1.05	4.93	8.25	9.08	10.05	8.42	6.74	6.14
	S	2.86	2.01	2.06	1.43	0.41	1.35	0.69	0.47	0.80	1.03

Note: "TI" indicates time interval, " $\varepsilon(\%)$ " indicates the percentage error, "S" indicates the system, and C1, C2, C3, C4, C5, and C6 indicate components 1, 2, 3, 4, 5, and 6, respectively.

sequence analysis results. It is seen that over part of the time period, sequence 2 is more probable than sequence 1. However, for the overall time period, sequence 1 has a higher probability than sequence 2.

All these results indicate that the proposed method is much more efficient than MCS for example 1. The proposed method can generate multiple outputs from a single analysis.

5.2 Parallel System: A Daniels System. A Daniels system subjected to a stochastic load $P(t)$ as shown in Fig. 6 is employed as the second example. The widths and heights of the two

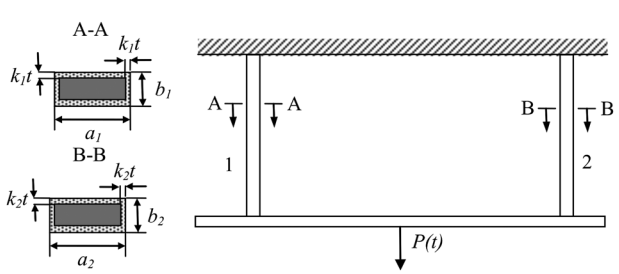

Fig. 6 A Daniels system with two components

Table 3 Parameters and variables in example 2

Variable	Mean	Standard deviation	Distribution	Autocorrelation
a_1	1.3 in.	0.01 in.	Normal	N/A
b_1	1.2 in.	0.01 in.	Normal	N/A
a_2	1.3 in.	0.05 in.	Normal	N/A
b_2	1.2 in.	0.05 in.	Normal	N/A
σ_{b1}, σ_{b2}	36 kpsi	0.36 kpsi	Normal	N/A
$P(t)$	85 kpsi	8 kpsi	Gaussian process	Eq. (43)

components decrease over time at rates of k_1 and k_2, respectively. Each component resists a load of $P(t)/2$. A failure occurs when both the components yield. The time-dependent system probability of failure of the system is given by

$$p_{f,s}(t_0, t_s) = \Pr\{g_1(\mathbf{X}, \mathbf{Y}(\chi), \chi) > 0 \cap g_2(\mathbf{X}, \mathbf{Y}(\tau), \tau) > 0, \exists \chi \text{ and } \tau \in [t_0, t_s]\} \quad (41)$$

where

$$g_i(\mathbf{X}, \mathbf{Y}(t), t) = P(t)/2 - (a_i - 2k_i t)(b_i - 2k_i t)\sigma_{bi}, \text{ where } i = 1, 2 \quad (42)$$

in which $[t_0, t_s] = [0, 10]$ years, $\mathbf{X} = [a_1, b_1, a_2, b_2, \sigma_{b1}, \sigma_{b2}]$, $\mathbf{Y}(t) = [P(t)]$, and $k_1 = 5 \times 10^{-4}$in./yr, $k_2 = 3 \times 10^{-4}$in./yr ; and σ_{b1} and σ_{b2} are the yield strengths of components 1 and 2, respectively. Table 3 illustrates the parameters in Eq. (42).

The autocorrelation function of the stochastic process $P(t)$ is given by

$$\rho^P(t_1, t_2) = \exp\left[-(t_2 - t_1)^2/\zeta^2\right] \quad (43)$$

where $\zeta = 0.5$ yr is the correlation length. The longer the time interval $t_2 - t_1$, the weaker is the autocorrelation.

We perform the time-dependent system reliability analysis using the proposed method as well as MCS. In MCS, the time interval is divided into 100 time instants. A total of 1×10^6 samples are generated at each time instant. The total number of function evaluations for MCS is 2×10^8. In the proposed method, the time interval is discretized into 23 time instants to satisfy the requirement of MSE of the surrogate models. The MPP searches are performed 46 times. The total number of function evaluations for the proposed method is **970**. Based on the eigenvalue and eigenvector analysis, the first 50 important features are used to model the equivalent random field. The time-dependent component and system probability of failure are analyzed based on the equivalent random field. Figures 7(*a*)–7(*c*) present the results comparison between the proposed method and the MCS. Similar as example 1, we also give the 95% prediction interval of the analysis results in Figs. 7(*a*)–7(*c*). Figure 7(*d*) gives the results of failure sequence analysis. The percentage errors of reliability analysis result over the time interval of interest are given in Table 2.

The results show that the proposed method can effectively approximate the time-dependent component and system probability of failure. For example 2, the failure sequence (2, 1) has a higher probability than the failure sequence (1, 2) for time period after 1.1 yr.

5.3 A Combined System: Six-Bar Indeterminate Truss. A six-bar indeterminate truss as presented in Fig. 8 is used as the third example. This example is modified from Ref. [30]. The failure of the truss is defined as the failure of any two bars. The system is therefore a combined system. Due to corrosion, the radii of the six bars decrease at the rates of $k_1 = 5 \times 10^{-4}$ in./yr, $k_2 = 3 \times 10^{-4}$ in./yr, $k_3 = 3 \times 10^{-4}$ in./yr, $k_4 = 3 \times 10^{-4}$ in./yr, $k_5 = 3 \times 10^{-4}$ in./yr, and $k_6 = 3 \times 10^{-4}$ in./yr, respectively.

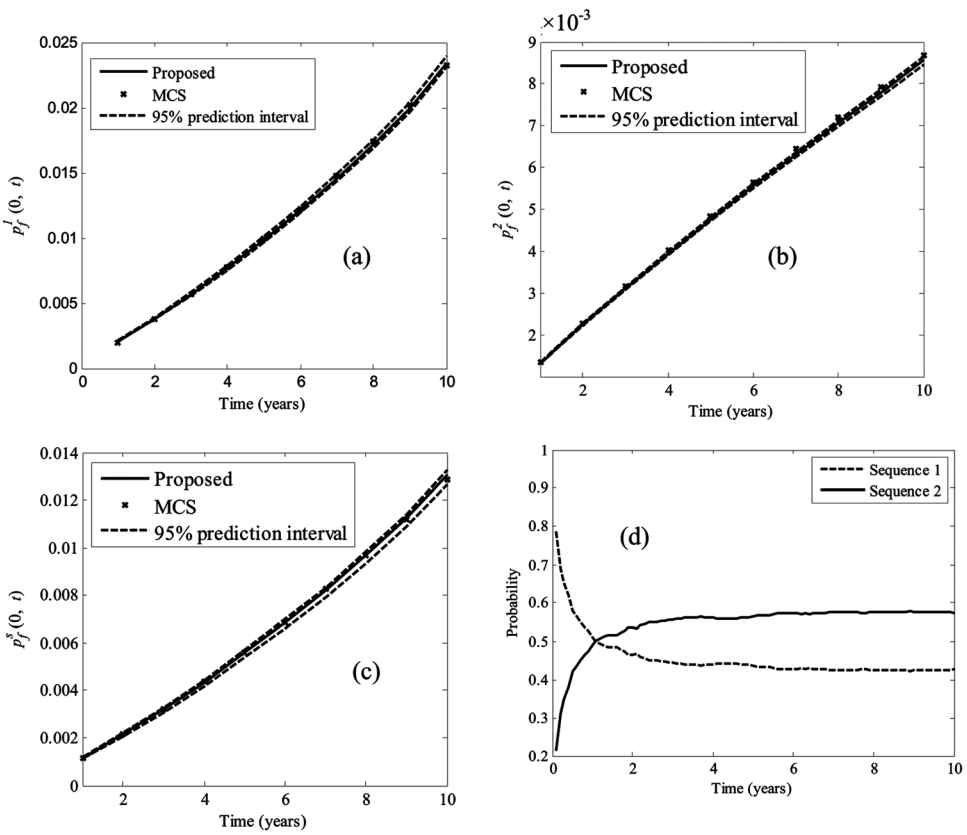

Fig. 7 Time-dependent system probability of failure and failure sequences of example 2: (*a*) component 1, (*b*) component 2, (*c*) system, and (*d*) failure sequences

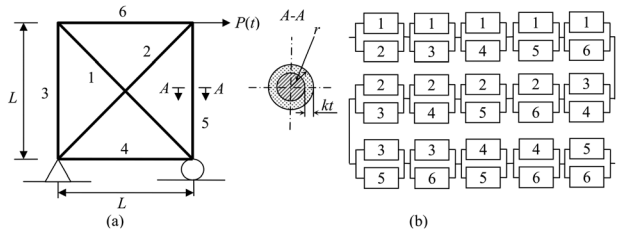

Fig. 8 (*a*) A six-bar indeterminate truss and (*b*) system configuration

The limit-state functions for the six bars are given as follows by assuming that the two diagonal members carry equal loads:

$$g_i(\mathbf{X}, \mathbf{Y}(t), t) = 0.707P(t) - \pi(r_i - k_i t)^2\sigma_i, \quad \text{for } i = 1, 2 \tag{44}$$

$$g_i(\mathbf{X}, \mathbf{Y}(t), t) = 0.5P(t) - \pi(r_i - k_i t)^2\sigma_i, \quad \text{for } i = 3, 4, 5, \text{ and } 6 \tag{45}$$

in which r_1 and r_2 follow $N(2.5, 0.05^2)$ in., r_3 to r_5 follow $N(2.3, 0.05^2)$ in., the yield strength of each bar (σ_1 to σ_6) is assumed to follow a normal distribution with mean of 36 kpsi and standard deviation of 3 kpsi, and $P(t)$ is a Gaussian stochastic process with mean of 700 kpsi, standard deviation of 70 kpsi, and correlation function given by

$$\rho^P(t_1, t_2) = \exp\left[-(t_2 - t_1)^2\right] \tag{46}$$

The overall limit-state function for time-dependent system reliability analysis is given by

$$p_f(t_0, t_e) = \Pr\left\{ \left(\bigcap_{i<j} [g_i(\mathbf{X}, \mathbf{Y}(t_i), t_i) > 0 \cup g_j(\mathbf{X}, \mathbf{Y}(t_j), t_j) > 0], \forall i, j = 1, 2, \ldots, 6 \right) \exists t_k, k = 1, 2, \cdots, 6 \in [t_0, t_e] \right\} \tag{47}$$

Similar to examples 1 and 2, we perform time-dependent system reliability analysis with the proposed method as well as MCS. In the proposed method, the equivalent random field is modeled

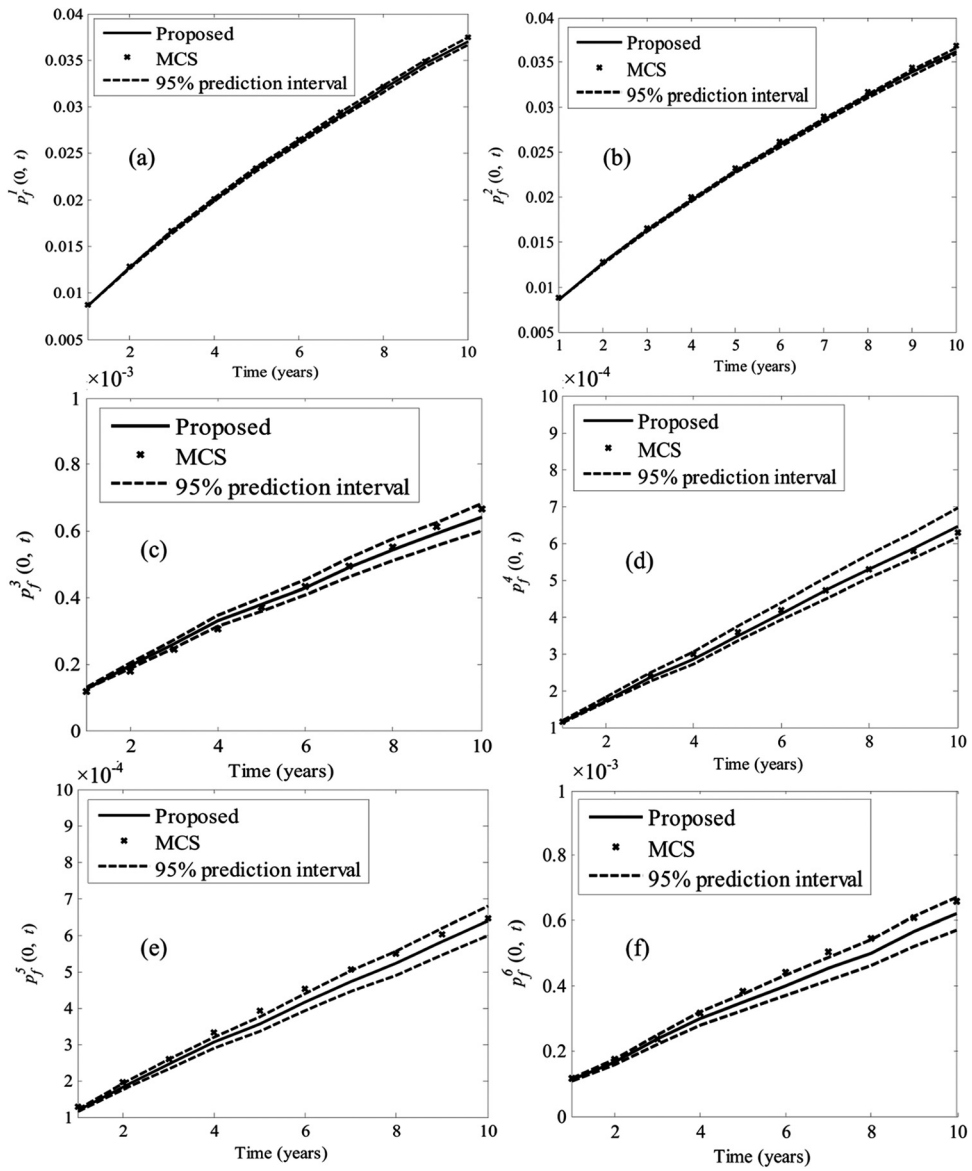

Fig. 9 Time-dependent component probability of failure: (*a*) component 1, (*b*) component 2, (*c*) component 3, (*d*) component 4, (*e*) component 5, and (*f*) component 6

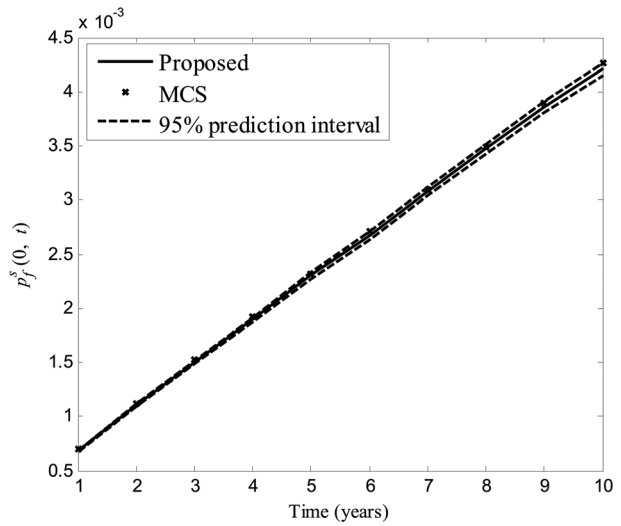

Fig. 10 Time-dependent system probability of failure

by the first 55 important features. The numbers of function evaluations for the proposed method and the MCS are **2005** and 1.2×10^9, respectively. Figure 9 shows the time-dependent component probability of failure of the six bars. Figure 10 gives the comparison of time-dependent system probability of failure.

The results indicate that the proposed method can effectively estimate the time-dependent system probability of failure even for a combined system. The failure sequence analysis results show two important failure sequences of example 3 are (1, 2) and (2, 1). Note that the stochastic loads used in examples 2 and 3 are all Gaussian stochastic processes. Since the developed method does not make any assumptions about distributions of random variables and stochastic processes, the developed method is still applicable when non-Gaussian stochastic processes are involved.

6 Conclusion

Previous studies on the time-dependent system reliability have investigated approximations by bounding the system reliability with the bivariate responses and by assuming the stochastic loading as a Poisson process. This paper overcomes both these approximations. Since the system responses are correlated over both components and time, this paper models them as a time-dependent discrete random field. The FORM is performed at specific points and components selected by design of experiments. Based on the FORM analysis, the system response is mapped into a discrete-continuous Gaussian nonstationary random field based on only the dominant important features. The time-dependent component probability of failure, system probability of failure, and important failure sequences are then obtained from the equivalent random field.

The proposed method does not require global optimization with respect to time, which is usually required in nested methods for time-dependent reliability analysis. The outputs of the proposed method are not just the system reliability for an interested time interval but also the entire time-dependent reliability curve up to that time interval. As byproducts of time-dependent system reliability analysis, the proposed method also obtains the time-dependent component reliability curves and the important failure sequences.

The proposed method still has two main limitations even if it is able to effectively perform time-dependent system reliability analysis for some problems: (1) The method is based on FORM. The errors of FORM will propagate to the results of time-dependent system reliability analysis. The proposed method is therefore limited to problems where the FORM is applicable. (2) The surrogate models need to be constructed for the mean and correlation functions of the equivalent random field. The accuracy of the surrogate models will affect the accuracy of the reliability analysis. This second issue relates to the number of training points, whereas the first issue needs generalization to situations where the FORM is not accurate.

References

[1] Andrieu-Renaud, C., Sudret, B., and Lemaire, M., 2004, "The PHI2 Method: A Way to Compute Time-Variant Reliability," Reliab. Eng. Syst. Saf., **84**(1), pp. 75–86.
[2] Hu, Z., and Du, X., 2012, "Reliability Analysis for Hydrokinetic Turbine Blades," Renewable Energy, **48**, pp. 251–262.
[3] Hu, Z., and Du, X., 2013, "Time-Dependent Reliability Analysis With Joint Upcrossing Rates," Struct. Multidiscip. Optim., **48**(5), pp. 893–907.
[4] Preumont, A., 1985, "On the Peak Factor of Stationary Gaussian Processes," J. Sound Vib., **100**(1), pp. 15–34.
[5] Singh, A., and Mourelatos, Z. P., 2010, "On the Time-Dependent Reliability of Non-Monotonic, Non-Repairable Systems," SAE Int. J. Mater. Manuf., **3**(1), pp. 425–444.
[6] Wang, Z., and Wang, P., 2012, "A Nested Extreme Response Surface Approach for Time-Dependent Reliability-Based Design Optimization," ASME J. Mech. Des., **134**(12), p. 121007.
[7] Hu, Z., and Du, X., 2015, "Mixed Efficient Global Optimization for Time-Dependent Reliability Analysis," ASME J. Mech. Des., **137**(5), p. 051401.
[8] Li, J., Chen, J.-b., and Fan, W.-l., 2007, "The Equivalent Extreme-Value Event and Evaluation of the Structural System Reliability," Struct. Saf., **29**(2), pp. 112–131.
[9] Jiang, C., Huang, X., Han, X., and Zhang, D., 2014, "A Time-Variant Reliability Analysis Method Based on Stochastic Process Discretization," ASME J. Mech. Des., **136**(9), p. 091009.
[10] Du, X., 2014, "Time-Dependent Mechanism Reliability Analysis With Envelope Functions and First-Order Approximation," ASME J. Mech. Des., **136**(8), p. 081010.
[11] Singh, A., Mourelatos, Z., and Nikolaidis, E., 2011, "Time-Dependent Reliability of Random Dynamic Systems Using Time-Series Modeling and Importance Sampling," SAE Int. J. Mater. Manuf., **4**(1), pp. 929–946.
[12] Wang, Z., Mourelatos, Z. P., Li, J., Baseski, I., and Singh, A., 2014, "Time-Dependent Reliability of Dynamic Systems Using Subset Simulation With Splitting Over a Series of Correlated Time Intervals," ASME J. Mech. Des., **136**(6), p. 061008.
[13] Hu, Z., and Du, X., 2015, "First Order Reliability Method for Time-Variant Problems Using Series Expansions," Struct. Multidiscip. Optim., **51**(1), pp. 1–21.
[14] Hagen, Ø., and Tvedt, L., 1991, "Vector Process Out-Crossing as Parallel System Sensitivity Measure," J. Eng. Mech., **117**(10), pp. 2201–2220.
[15] Song, J., and Der Kiureghian, A., 2006, "Joint First-Passage Probability and Reliability of Systems Under Stochastic Excitation," J. Eng. Mech., **132**(1), pp. 65–77.
[16] Radhika, B., Panda, S., and Manohar, C., 2008, "Time Variant Reliability Analysis of Nonlinear Structural Dynamical Systems Using Combined Monte Carlo Simulations and Asymptotic Extreme Value Theory," Comput. Model. Eng. Sci., **27**(1–2), pp. 79–110.
[17] Dey, A., and Mahadevan, S., 2000, "Reliability Estimation With Time-Variant Loads and Resistances," J. Struct. Eng., **126**(5), pp. 612–620.
[18] Ditlevsen, O., 1979, "Narrow Reliability Bounds for Structural Systems," J. Struct. Mech., **7**(4), pp. 453–472.
[19] Hohenbichler, M., and Rackwitz, R., 1983, "First-Order Concepts in System Reliability," Struct. Saf., **1**(3), pp. 177–188.
[20] Dey, A., and Mahadevan, S., 1998, "Ductile Structural System Reliability Analysis Using Adaptive Importance Sampling," Struct. Saf., **20**(2), pp. 137–154.
[21] Youn, B. D., and Wang, P., 2009, "Complementary Intersection Method for System Reliability Analysis," ASME J. Mech. Des., **131**(4), p. 041004.
[22] Wang, Z., and Wang, P., 2015, "An Integrated Performance Measure Approach for System Reliability Analysis," ASME J. Mech. Des., **137**(2), p. 021406.
[23] Sudret, B., and Der Kiureghian, A., 2000, "Stochastic Finite Element Methods and Reliability: A State-of-the-Art Report," Department of Civil and Environmental Engineering, University of California, Berkeley, CA, Technical Report No. UCB/SEMM-2000/08.
[24] Amsallem, D., and Farhat, C., 2012, "Stabilization of Projection-Based Reduced-Order Models," Int. J. Numer. Methods Eng., **91**(4), pp. 358–377.
[25] Xi, Z., Youn, B. D., and Hu, C., 2010, "Random Field Characterization Considering Statistical Dependence for Probability Analysis and Design," ASME J. Mech. Des., **132**(10), p. 101008.
[26] Santner, T. J., Williams, B. J., and Notz, W., 2003, *The Design and Analysis of Computer Experiments*, Springer, New York.
[27] Swiler, L. P., Hough, P. D., Qian, P., Xu, X., Storlie, C., and Lee, H., 2014, "Surrogate Models for Mixed Discrete-Continuous Variables," Constraint Programming and Decision Making, Springer, Cham, Switzerland, pp. 181–202.
[28] Wang, P., Hu, C., and Youn, B. D., 2011, "A Generalized Complementary Intersection Method (GCIM) for System Reliability Analysis," ASME J. Mech. Des., **133**(7), p. 071003.
[29] Zhang, J., and Du, X., 2011, "Time-Dependent Reliability Analysis for Function Generator Mechanisms," ASME J. Mech. Des., **133**(3), p. 031005.
[30] McDonald, M., and Mahadevan, S., 2008, "Design Optimization With System-Level Reliability Constraints," ASME J. Mech. Des., **130**(2), p. 021403.